AGU PUBLICATIONS

Geophysical Research Letters

RESEARCH LETTER
10.1002/2014GL062584

Key Points:
- The years 2007 and 2010 were major fire years in tropical South America
- Lower than expected 2010 CO emissions despite a once-in-a-century drought
- The 2010 fire carbon losses were likely low due to reduced biomass combustion rates

Supporting Information:
- Text S1, Figures S1–S4, and Tables S1–S3

Correspondence to:
A. A. Bloom,
abloom@jpl.nasa.gov

Citation:
Bloom, A. A., J. Worden, Z. Jiang, H. Worden, T. Kurosu, C. Frankenberg, and D. Schimel (2015), Remote-sensing constraints on South America fire traits by Bayesian fusion of atmospheric and surface data, *Geophys. Res. Lett.*, *42*, 1268–1274, doi:10.1002/2014GL062584.

Received 19 NOV 2014
Accepted 18 JAN 2015
Accepted article online 23 JAN 2015
Published online 26 FEB 2015

Remote-sensing constraints on South America fire traits by Bayesian fusion of atmospheric and surface data

A. Anthony Bloom[1], John Worden[1], Zhe Jiang[1], Helen Worden[2], Thomas Kurosu[1], Christian Frankenberg[1], and David Schimel[1]

[1]Jet Propulsion Laboratory, California Institute of Technology, Pasadena, California, USA, [2]Atmospheric Chemistry Division, National Center for Atmospheric Research, Boulder, Colorado, USA

Abstract Satellite observations reveal substantial burning during the 2007 and 2010 tropical South America fire season, with both years exhibiting similar total burned area. However, 2010 CO fire emissions, based on satellite CO concentration measurements, were substantially lower (−28%), despite the once-in-a-century drought in 2010. We use Bayesian inference with satellite measurements of CH_4 and CO concentrations and burned area to quantify shifts in combustion characteristics in 2010 relative to 2007. We find an 88% probability in reduced combusted biomass density associated with the 2010 fires and an 82% probability of lower fire carbon losses in 2010 relative to 2007. Higher combustion efficiency was a smaller contributing factor to the reduced 2010 CO emissions. The reduction in combusted biomass density is consistent with a reduction (4–6%) in Global Ozone Monitoring Experiment 2 solar-induced fluorescence (a proxy for gross primary production) during the preceding months and a potential reduction in biomass (≤8.3%) due to repeat fires.

1. Introduction

Tropical fire carbon (C) losses, largely in the form of CO_2, CO, and CH_4, amount to a significant portion of the global carbon budget. Tropical South America fires accounted for 5–35% of annual tropical fire CO_2 emissions during 2001–2011 (Global Fires Emissions Database) [*van der Werf et al.*, 2010]. Larger fire C losses typically occur during drier years [*Chen et al.*, 2013b]. For example, during the once-in-a-century 2010 Amazon drought [*Lewis et al.*, 2011], the combined effect of larger fires and reduced terrestrial C uptake resulted in a reversal of the net atmosphere-to-land C flux [*Gatti et al.*, 2014]. Fires can also have long-term effects on C cycling, resulting from increased tree mortality and shifting toward fire-resilient species [*Brando et al.*, 2014].

Emissions of CO_2, CO, and CH_4 from fires are governed by the amount of available biomass C, the fraction of biomass C combusted (combustion completeness), and the fraction of combusted C emitted as CO_2 (combustion efficiency). Droughts can lead to changes in biomass burning traits, including reductions in fuel load [*Randerson et al.*, 2005; *Chen et al.*, 2013a] and fuel moisture [*Hély et al.*, 2003], which in turn will influence overall combustion efficiency and completeness [*Korontzi et al.*, 2003; *Hély et al.*, 2003; *Soares Neto et al.*, 2009]; these shifts can significantly alter large-scale fire C loss rates. Overall, placing top-down constraints on combustion characteristics and their interannual variations is essential to better quantify continental-scale terrestrial C exchange.

The relative scarcity of large-scale, repeat measurements of atmospheric CO_2 has posed a significant barrier to estimating C losses from tropical fires. CO and CH_4 are the next largest gaseous forms of C loss from fires [*Andreae and Merlet*, 2001]. Based on in situ measurements of the ratios of CO_2 to CO and CH_4 (or CO_2 : CO : CH_4) within fire plumes, CO and CH_4 can provide a constraint on total C emissions. However, CO and CH_4 emission factors vary among major land cover types [*Andreae and Merlet*, 2001; *Akagi et al.*, 2011], and associated estimates of total C losses will inherently remain highly uncertain. Observations of burned area provide an independent constraint on fire C losses. Within burned areas, typically a high fraction of litter and foliar C is combusted, while coarser aboveground woody C is only partially combusted [*Ward et al.*, 1996; *Prasad et al.*, 2001]. The overall combustion completeness also varies as a result of fuel moisture [*Hély et al.*, 2003] and fuel types [*Korontzi et al.*, 2003; *Soares Neto et al.*, 2009] among other attributes. As a result, biomass density and combustion completeness remain dominant sources of uncertainty in bottom-up C loss estimates. Ultimately, trace gas, biomass, and burned area constraints can be used together to reduce uncertainties on fire C loss rates.

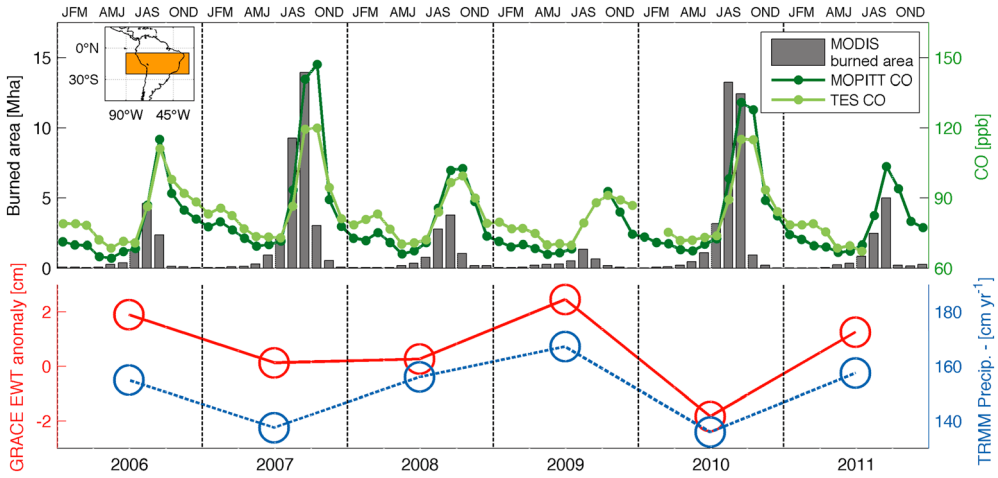

Figure 1. (top) Monthly MODIS burned area (dark grey), MOPITT CO (dark green), and TES CO (light green) during 2006–2011 within the study area. (inset) Map showing the tropical South America study area. (bottom) Annual mean GRACE equivalent water height (EWT) and TRMM total precipitation within the study area.

2. Remote-Sensing Constraints

Our study is focused on tropical South America (study region: 25°S–5°S, 90°W–30°W): according to the Global Fires Emissions Database (GFEDv3) [*van der Werf et al.*, 2010], biomass burning within the study region amounts to 92% of total South America emissions during 2001–2011. Burned area within this region peaks during the dry season (July–October; Figure 1). We find large-scale agreements between the timing and magnitude of MODIS (Moderate Resolution Imaging Spectroradiometer) burned area [*Giglio et al.*, 2013], TES (Tropospheric Emission Spectrometer) CO retrievals (tes.jpl.nasa.gov), and MOPITT (Measurements Of Pollution In The Troposphere) CO V6J retrievals [*Worden et al.*, 2010; *Deeter et al.*, 2014]. Interannual variations in Tropical Rainfall Measuring Mission (TRMM) precipitation retrievals [*Huffman et al.*, 2007] and Gravity Recovery and Climate Experiment (GRACE) water storage retrievals [*Landerer and Swenson*, 2012] are broadly consistent with the dry-season CO and burned area magnitudes.

Two of the major fire years during this time period (2007 and 2010) exhibited similar burned areas (Figure 2a). However, in contrast to recent major droughts in 2005 and 2010 [*Lewis et al.*, 2011; *Gloor et al.*, 2013], 2007 was not a major drought year. The total aboveground biomass within the 2010 burned areas [*Saatchi et al.*, 2011] is 13% higher, and GFEDv3 bottom-up emission estimates amount to higher CO emissions (+24%) and higher total C loss (+23%) from 2010 fires, relative to 2007 [*van der Werf et al.*, 2010]. However, TES and MOPITT column-integrated CO data (Figure 1) do not exhibit enhanced CO concentrations in 2010, relative to 2007. Moreover, CO inverse emission estimates based on MOPITT CO observations are 28% lower in 2010, relative to 2007 (Figure 2b). Details on the inverse CO emission estimates are provided in Text S1 of the supporting information. Similarly, we find no significant enhancement in 2010 Ozone Monitoring Instrument (OMI) NO_2 concentrations relative to 2007 (Figure S3 in the supporting information).

We use the *Worden et al.* [2013a, 2013b] approach to determine fire plume CH_4/CO ratios from Aura TES column-integrated CO and CH_4 observations over the study region. We find a higher 2010 CH_4/CO (0.11 g CH_4 g^{-1} CO) relative to 2007 (0.07–0.09 g CH_4 g^{-1} CO; see the supporting information for details): this increase supports the explanation of a higher forest fire contribution to total CH_4 and CO emissions in 2010, because forest fires typically have a higher CH_4-to-CO ratio (i.e., higher CH_4/CO) relative to savanna and grassland fires [*Andreae and Merlet*, 2001] (see Figure 2c). However, the relative increase in forest fire emissions alone cannot account for a 28% decrease in CO emissions without a sizeable decrease in savanna and agricultural fire CO emissions. Likewise, elevated CH_4/CO in 2010 cannot be solely attributed to lower CO emission rates due to lower fuel moisture (i.e., higher combustion efficiency), as CH_4 and CO emissions factors are positively correlated [*Korontzi et al.*, 2003; *Soares Neto et al.*, 2009].

Therefore, lower than expected CO emissions in 2010 may have occurred as a result of a combined higher forest fire contribution and lower CO emission factors: a large-scale shift from smoldering to flaming fires

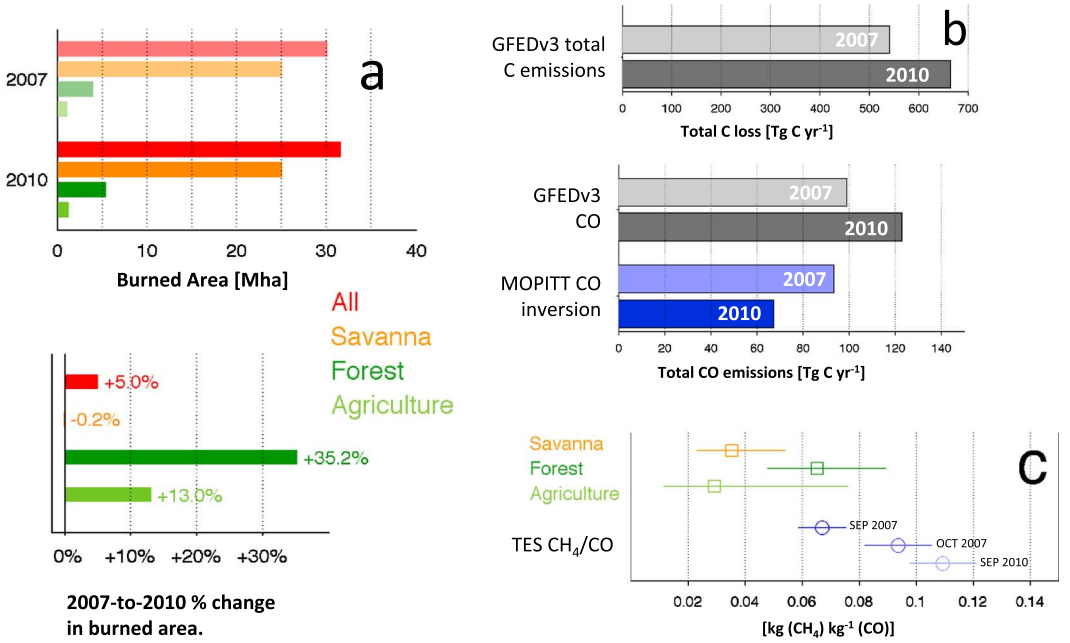

Figure 2. (a) Savanna, forest, agriculture and total burned area and 2007-to-2010 percent changes in total burned area within the study region. (b) Bottom-up (GFEDv3) 2007 and 2010 total fire C emissions and bottom-up (GFEDv3) and top-down (MOPITT) estimates of 2007 and 2010 fire CO within the study area. (c) Land cover-specific CH_4/CO mass ratios and associated uncertainties, for savanna, forest, and agriculture fires emissions; TES CH_4/CO ratios based on monthly TES column-integrated CO and CH_4 concentrations within the study area.

[*Soares Neto et al.*, 2009] may have resulted in increased combustion efficiency (i.e., lower CO emission rates). Alternatively, a 2010 decrease in combusted biomass density (biomass density × combustion completeness) may have resulted in both lower CO emissions and lower total fire C loss. A reduction in biomass may have occurred as a result of reduced gross primary production (GPP) during the 2010 wet season [*Lewis et al.*, 2011], which in turn could lead to a reduction in easily combustible fuel during the dry season [*Randerson et al.*, 2005; *Chen et al.*, 2013a].

To establish why in 2010, relative to 2007, burned area was higher (+5%) while 2010 CO emissions are lower (−28%), we use Bayesian inference to determine the probability of four hypotheses concerning a 2007-to-2010 increase/decrease in combustion efficiency and combusted biomass density: the hypotheses are summarized in Table 1. By quantifying the probability for each hypothesis, we can identify the likely underlying factors leading to greater burned area and less CO emissions in 2010, relative to 2007. Moreover, by quantifying the increase/decrease in combusted biomass density and combustion efficiency, we can quantify the difference between 2007 and 2010 fire C losses. We bring (a) MOPITT CO concentrations, (b) TES CH_4/CO ratios, (c) MODIS burned area, (d) aboveground total biomass [*Saatchi et al.*, 2011], and (e) land cover type CO and CH_4 emission factor prior information [*Andreae and Merlet*, 2001] together in a Bayesian inference framework to quantify changes in combusted biomass density (henceforth CBD = [combusted biomass]/[area]; unit in kg C m^{-2}), modified combustion efficiency (henceforth MCE = $[CO_2]/[CO_2 + CO + CH_4]$; unit in [kg C] $[kg C]^{-1}$), and total South America fire C losses in 2007 and 2010.

Table 1. Hypotheses 1–4[a]

Hypotheses	Change in 2010 Combusted Biomass Density (CBD) and Combustion Efficiency (MCE), Relative to 2007
H1	Decrease in CBD and decrease in MCE.
H2	Decrease in CBD and increase in MCE.
H3	Increase in CBD and increase in MCE.
H4	Increase in CBD and decrease in MCE.

[a]Hypotheses 1–4 outline all combinations of combusted biomass density (CBD: [combusted biomass]/[area]; unit in kg m^{-2}) and modified combustion efficiency (MCE: $[CO_2]/[CO_2 + CO + CH_4]$; unit in (kg C) $(kg C)^{-1}$) changes between 2007 and 2010.

3. Estimates of Burning Coefficients

We express fire C fluxes of trace gas species s from land cover type b, $F_{s,b}$, as

$$F_{s,b} = A_b \times CBD_b \times E_{s,b} \quad (1)$$

where A_b, CBD_b, and E_b are the burned area (m^2), combusted biomass density (kg C m^{-2}) within each land cover type b, and $E_{s,b}$ is the corresponding carbon emission factor (kg C species per kg C combusted) for each trace gas species s within each land cover type b. CBD_b can be expressed as

$$CBD_b = C_b \times B_b \tag{2}$$

where C_b and B_b are the combustion completeness and biomass density in land cover type b, respectively. We express modified combustion efficiency (MCE_b) as

$$MCE_b = 1 - E_{CO,b} - E_{CH_4,b} \tag{3}$$

given that biomass burning C losses other than CH_4, CO_2, and CO emissions are negligible [*Andreae and Merlet*, 2001].

We determine the total burned area in 2007 and 2010 (A_b) during the fire season (May–December) for each land cover type from the *Giglio et al*. [2013] MODIS burned area 0.25° × 0.25° gridded product: based on the burned area land cover types, we determine the A_b for three major land cover type groups, savannas and grasslands, forests, and agriculture. We treat CBD_b^y and $E_{s,b}^y$ (for s = [CO, CH_4]; for b = [(1) savanna and grasslands, (2) forest, and (3) agriculture]; for y = [2007, 2010]) as unknown quantities (henceforth parameter vector **x**). Based on the study region-scale observations **O**, which consist of CO and CH_4 observational constraints (total May–December 2007, 2010 MOPITT-derived CO emissions, and monthly TES CH_4/CO ratios), we use Bayesian inference to derive the probability density function of **x** given **O**, p(**x**|**O**), as follows:

$$p(\mathbf{x}|\mathbf{O}) \propto p(\mathbf{O}|\mathbf{x})\ p(\mathbf{x}) \tag{4}$$

where p(**O**|**x**) is the probability of **O** given **x** and p(**x**) is the prior probability of **x**. For a given parameter vector **x**, p(**O**|**x**) is determined by comparing study area-integrated fluxes ($\sum_{b=1}^{3} F_{CO,b}$ and $\sum_{b=1}^{3} F_{CH_4,b}$) against TES CH_4/CO and total MOPITT-derived CO emission estimates and their associated uncertainty characteristics. For a given parameter vector **x**, p(**x**) consists of prior constraints on CBD_b^y and $E_{s,b}^y$ and their associated uncertainty characteristics. We use a Metropolis Hastings Markov Chain Monte Carlo approach (MHMCMC) [e.g., *Ziehn et al*., 2012; *Bloom and Williams*, 2014] to derive 2×10^5 samples of **x**; based on their distribution, we derive the probability density functions of CBD_b^y and $E_{s,b}^y$. Details on the observational and prior constraints, their associated uncertainties, and the MHMCMC approach are included in the supporting information.

From 2×10^5 samples of CBD_b^y and $E_{s,b}^y$, we determine the region-wide overall combusted biomass density (CBD^y) and modified combustion efficiency (MCE^y) for years y (y = 2007, 2010), as follows:

$$CBD^y = \frac{\sum_{b=1}^{3} A_b^y\ CBD_b^y}{\sum_{b=1}^{3} A_b^y}, \quad MCE^y = \frac{\sum_{b=1}^{3} \left(1 - E_{CH_4,b}^y - E_{CO,b}^y\right) A_b^y CBD_b^y}{\sum_{b=1}^{3} A_b^y CBD_b^y}, \tag{5}$$

We also determine the probability density function of the carbon fluxes for each vegetation type based on the 2×10^5 CBD_b samples. We calculate total C losses F_C as the overall sum of total C losses ($A_b \times CBD_b$) from savanna, forest, and agriculture fires. We determine individual land cover type and region-wide probabilities for hypotheses 1–4 as follows:

$$\text{Probability of } H_N = [\text{No. of samples } \mathbf{x} \text{ where } H_N \text{ is true}] / \left[2 \times 10^5\right] \times 100\%. \tag{6}$$

4. Combusted Biomass Density, Efficiency, and C Losses

Table 2 describes the probability of 2007-to-2010 changes in combusted biomass density [CBD: g C combusted/burned area] and modified combustion efficiency [MCE: kg C (CO_2)/kg C ($CO + CH_4 + CO_2$)]. For example, there is a 25% probability that both CBD and MCE increased in 2010 within savanna fires, as shown in the "H1" row and "savanna" column of Table 2. Within the whole study area, we find that lower CBD and higher MCE—hypothesis 2—is the most probable cause for lower CO emissions and larger burned area in 2010, relative to 2007 (H2: 60%; see Figure 3). In particular, a change in forest and savanna fire

Table 2. Probability of Hypotheses 1–4[a]

		Savanna	Forests	Agriculture	Whole Study Area
Hypothesis	2010–2007 CBD and MCE Change	Hypothesis Probability			
H1	CBD ↓ MCE ↓	25%	19%	26%	**28**%
H2	CBD ↓ MCE ↑	47%	55%	28%	**60**%
H3	CBD ↑ MCE ↑	19%	17%	24%	**12**%
H4	CBD ↑ MCE ↓	8%	9%	22%	**0**%

[a]Probabilities of hypotheses 1–4 (see Table 1) based on Bayesian inference of combusted biomass density (CBD) and modified combustion efficiency (MCE): land-surface and atmospheric constraints on fire C emissions were used to calculate optimal 2007 and 2010 CBD and MCE values.

characteristics likely explains the reduced CO emissions, with 47% and 55% probabilities that there were both a reduction in CBD and an increase in MCE within these fires. While it is possible that CBD increased and MCE decreased within any of the three regions, there is a 0% probability that all three regions exhibited this change in fire characteristics. The probability density function of 2007-to-2010 changes in MCE and CBD is shown in Figure 3. We could not resolve the probable changes in agricultural combustion traits (H1: 26%, H2: 28%, H3: 24%, and H4: 22%), likely because these is a relatively small contribution to total C emissions from agricultural fires in both years (A_{agr} was 20% and 22% of total burned area in 2007 and 2010).

The hypotheses 1–4 probabilities depend on the uncertainties for the combusted biomass density and emission factor parameters in equation (1) (CBD_b and $E_{s,b}$), as well as the observation uncertainties; these are reported in the supporting information. The uncertainties that most strongly affect these outcomes are those related to the mean and the 2007-to-2010 change in equation (1) parameters. For example, we currently assume a one-sigma probability that fire characteristics will change by less than a factor of 2 between 2007 and 2010. This is a conservative estimate of interannual variations in fire characteristics, based on the seasonal range of reported combustion factor and efficiency measurements [e.g., *Korontzi et al*., 2003; *Hély et al*., 2003], as we are not aware of any interannual measurements of these parameters. However, even when we increase this uncertainty by a factor of 2, our overall conclusions remain unchanged (Table S3 in the supporting information). Additional potential sources of error in our simple model (equation (1)) include biases in MODIS-derived total fire season burned area and land cover classifications [*Giglio et al*., 2013]. We also note the potential effect of seasonal changes in CBD and MCE: biomass burning combustion factor and efficiency can vary significantly on monthly time scales [*Korontzi*, 2005].

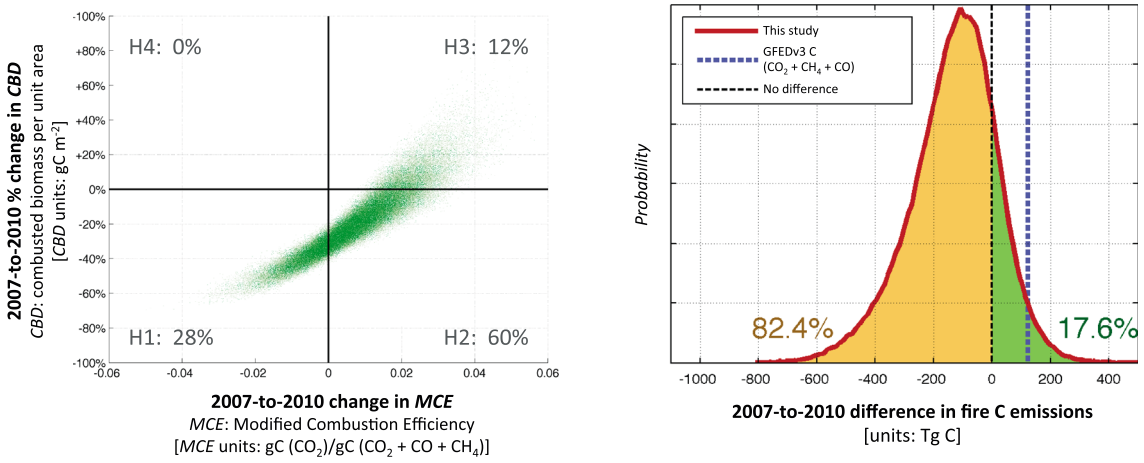

Figure 3. (left) Probability distribution of 2007-to-2010 combusted biomass density change (CBD, *y* axis) and combustion efficiency change (MCE, *x* axis) within the study area. Positive changes in MCE correspond to a decrease in CO emission factors between 2007 and 2010. The probabilities of hypotheses 1–4 (Table 1) are shown within each quadrant. (right) The 2007-to-2010 difference in biomass burning total C emissions based on optimized CBD values, in comparison to bottom-up 2007-to-2010 total C emissions difference (based on total GFEDv3 $CO_2 + CO + CH_4$ from savanna, forest, and agriculture fires); the orange/green numbers denote the top-down probability of less/more total C emissions from 2010 fires relative to 2007 fires.

5. Discussion and Implications

If we combine the outcomes for the change in combusted biomass density (g C combusted/burned area) and modified combustion efficiency ($CO_2/[CO + CH_4 + CO_2]$) with the change in burned area (equation (1)), we find that total C emissions were likely lower by ~119 Tg C in 2010 relative to 2007 (Figure 3). However, there is a non-zero (17.6%) probability of an increase in carbon emissions. In contrast, the bottom-up (or GFEDv3) fire emissions were higher by +123 Tg C in 2010, relative to 2007.

For the whole study area, the probability of a 2007-to-2010 combusted biomass density reduction (H1 and H2) is 88%, and the probability of a modified combustion efficiency increase (H2 and H3) is 72% (Figure 3). The 2007-to-2010 increase in modified combustion efficiency (median increase = +0.01) is consistent with observed increases in combustion efficiency due to drier fuel conditions [*Korontzi et al*., 2003; *Soares Neto et al*., 2009]. The median 2007-to-2010 combusted biomass density reduction is 22%: based on equation (2), this reduction corresponds to either (a) a 22% reduction in biomass density or (b) a 22% reduction in the combustion completeness or (c) a combined change in both. We next discuss the potential causes of 2007-to-2010 changes in biomass and/or combustion completeness.

Reduced productivity during the regional drought in 2010 may have led to a reduction in biomass available for combustion: as a large proportion of biomass loss from fires is derived from leaf and wood litter C, a reduction in the preceding wet season GPP and corresponding fuel load [e.g., *Randerson et al*., 2005] is a viable cause for a reduction of CO and fire C losses in 2010 shown in Figure 3. We find a 4–6% reduction in Global Ozone Monitoring Experiment (GOME)-2 measurements of solar-induced fluorescence (henceforth SIF) [*Joiner et al*., 2013] in 2010 relative to 2007 during the time period preceding the major fires (February–June) within the study area (see the supporting information). SIF is a proxy for GPP [*Frankenberg et al*., 2011], which in turn determines the fuel load during the subsequent fire season [e.g., *Randerson et al*., 2005]. Reduction in biomass density between 2007 and 2010 may have also occurred due to repeat fires and deforestation; we estimate that repeat fires could amount for up to an 8.3% reduction in biomass within burned areas between 2007 and 2010 (see the supporting information).

Combustion completeness (the fraction of biomass burned) is typically expected to increase as a result of drier conditions [*Hély et al*., 2003; *Korontzi*, 2005; *van der Werf et al*., 2010]. However, a reduction in GPP, leading to less combustible fuel, could in turn lead to diminished fire persistence [e.g., *Giglio et al*., 2006], therefore effectively suppressing large-scale combustion completeness within burned areas. Overall reductions in biomass and combustion completeness are both possible explanations for a reduction in combusted biomass density, and we currently do not have the large-scale constraints needed to differentiate between the two. We therefore require further data constraints to better quantify trends in fire C losses and biomass burning characteristics.

Orbiting Carbon Observatory-2 XCO_2 data [*Crisp et al*., 2008] will place stronger constraints on the interannual carbon emissions from fires. For example, both a 2007-to-2010 increase and decrease of combusted biomass density are possible, as shown in Table 2. Currently combusted biomass density is indirectly constrained by the CO and CH_4 from MOPITT and TES, but these trace gases represent 2–9% of carbon in biomass burning emissions. XCO_2-derived CO_2 fluxes would place a stronger constraint on combusted biomass density. Similarly, XCO_2 data from biomass burning plumes would place stronger constraints on combustion efficiency. Satellite-derived aboveground biomass data, such as the future Global Ecosystem Dynamics Investigation Lidar and BIOMASS missions [*Krainak et al*., 2012; *Hélière et al*., 2014], can also be used to deconvolve changes in biomass density and combustion completeness.

Acknowledgments

Part of this research was carried out at the Jet Propulsion Laboratory, California Institute of Technology, under a contract with the National Aeronautics and Space Administration. TES CH_4 and CO data products are available at tes.jpl.nasa.gov. The MODIS burned area product was obtained from modis-fire.umd.edu. The NCAR MOPITT project is supported by the National Aeronautics and Space Administration (NASA) Earth Observing System (EOS) Program. We are grateful for feedback from F. Landerer and J. Joiner on our use of GRACE and GOME-2 data. This research was funded by NASA ROSES CSS proposal 13-CARBON13_2-0071.

The Editor thanks two anonymous reviewers for their assistance in evaluating this paper.

References

Akagi, S. K., R. J. Yokelson, C. Wiedinmyer, M. J. Alvarado, J. S. Reid, T. Karl, J. D. Crounse, and P. O. Wennberg (2011), Emission factors for open and domestic biomass burning for use in atmospheric models, *Atmos. Chem. Phys.*, *11*(9), 4039–4072, doi:10.5194/acp-11-4039-2011.

Andreae, M. O., and P. Merlet (2001), Emission of trace gases and aerosols from biomass burning, *Global Biogeochem. Cycles*, *15*(4), 955–966, doi:10.1029/2000GB001382.

Bloom, A. A., and M. Williams (2014), Constraining ecosystem carbon dynamics in a data-limited world: Integrating ecological "common sense" in a model-data-fusion framework, *Biogeosci. Discuss.*, *11*(8), 12,733–12,772, doi:10.5194/bgd-11-12733-2014.

Brando, P. M., et al. (2014), Abrupt increases in Amazonian tree mortality due to drought–fire interactions, *Proc. Natl. Acad. Sci. U.S.A.*, *111*(17), 6347–6352, doi:10.1073/pnas.1305499111.

Chen, Y., D. C. Morton, Y. Jin, G. J. Collatz, P. S. Kasibhatla, G. R. van der Werf, R. S. DeFries, and J. T. Randerson (2013a), Long-term trends and interannual variability of forest, savanna and agricultural fires in South America, *Carbon Manage.*, *4*(6), 617–638, doi:10.4155/cmt.13.61.

Chen, Y., I. Velicogna, J. S. Famiglietti, and J. T. Randerson (2013b), Satellite observations of terrestrial water storage provide early warning information about drought and fire season severity in the Amazon, *J. Geophys. Res. Biogeosci.*, *118*, 495–504, doi:10.1002/jgrg.20046.

Crisp, D., P. L. DeCola, and C. E. Miller (2008), NASA Orbiting Carbon Observatory: Measuring the column averaged carbon dioxide mole fraction from space, *J. Appl. Remote Sens.*, *2*(1), 023508, doi:10.1117/1.2898457.

Deeter, M. N., S. Martínez-Alonso, D. P. Edwards, L. K. Emmons, J. C. Gille, H. M. Worden, C. Sweeney, J. V. Pittman, B. C. Daube, and S. C. Wofsy (2014), The MOPITT version 6 product: Algorithm enhancements and validation, *Atmos. Meas. Tech. Discuss.*, *7*(6), 6113–6139, doi:10.5194/amtd-7-6113-2014.

Frankenberg, C., et al. (2011), New global observations of the terrestrial carbon cycle from GOSAT: Patterns of plant fluorescence with gross primary productivity, *Geophys. Res. Lett.*, *38*, L17706, doi:10.1029/2011GL048738.

Gatti, L. V., et al. (2014), Drought sensitivity of Amazonian carbon balance revealed by atmospheric measurements, *Nature*, *506*(7486), 76–80, doi:10.1038/nature12957.

Giglio, L., G. R. Van der Werf, J. T. Randerson, G. J. Collatz, and P. Kasibhatla (2006), Global estimation of burned area using MODIS active fire observations, *Atmos. Chem. Phys.*, *6*(4), 957–974, doi:10.5194/acp-6-957-2006.

Giglio, L., J. T. Randerson, and G. R. van der Werf (2013), Analysis of daily, monthly, and annual burned area using the Fourth-Generation Global Fire Emissions Database (GFED4), *J. Geophys. Res. Biogeosci.*, *118*, 317–328, doi:10.1002/jgrg.20042.

Gloor, M., R. J. W. Brienen, D. Galbraith, T. R. Feldpausch, J. Schöngart, J.-L. Guyot, J. C. Espinoza, J. Lloyd, and O. L. Phillips (2013), Intensification of the Amazon hydrological cycle over the last two decades, *Geophys. Res. Lett.*, *40*, 1729–1733, doi:10.1002/grl.50377.

Hélière, F., F. Fois, M. Arcioni, P. Bensi, M. Fehringer, and K. Scipal (2014), Biomass P-band SAR interferometric mission selected as 7th Earth Explorer Mission, EUSAR 2014, in *Proceedings of 10th European Conference on Synthetic Aperture Radar*, pp. 1–4, VDE, Berlin.

Hély, C., S. Alleaume, R. J. Swap, and C. O. Justice (2003), SAFARI-2000 characterization of fuels, fire behavior, combustion completeness, and emissions from experimental burns in infertile grass savannas in western Zambia, *J. Arid. Environ.*, *54*(2), 381–394, doi:10.1006/jare.2002.1097.

Huffman, G. J., D. T. Bolvin, E. J. Nelkin, D. B. Wolff, R. F. Adler, G. Gu, Y. Hong, K. P. Bowman, and E. F. Stocker (2007), The TRMM Multisatellite Precipitation Analysis (TMPA): Quasi-global, multiyear, combined-sensor precipitation estimates at fine scales, *J. Hydrometeorol.*, *8*(1), 38–55, doi:10.1175/JHM560.1.

Joiner, J., L. Guanter, R. Lindstrot, M. Voigt, A. P. Vasilkov, E. M. Middleton, K. F. Huemmrich, Y. Yoshida, and C. Frankenberg (2013), Global monitoring of terrestrial chlorophyll fluorescence from moderate-spectral-resolution near-infrared satellite measurements: Methodology, simulations, and application to GOME-2, *Atmos. Meas. Tech.*, *6*(10), 2803–2823, doi:10.5194/amt-6-2803-2013.

Korontzi, S. (2005), Seasonal patterns in biomass burning emissions from southern African vegetation fires for the year 2000, *Global Change Biol.*, *11*, 1680–1700, doi:10.1111/j.1365-2486.2005.001024.x.

Korontzi, S., et al. (2003), Seasonal variation and ecosystem dependence of emission factors for selected trace gases and PM2.5 for southern African savanna fires, *J. Geophys. Res.*, *108*(D24), 4758, doi:10.1029/2003JD003730.

Krainak, M. A., et al. (2012), Laser Transceivers for Future NASA Missions, *Proc. SPIE*, vol. 8381, 83810Y, Laser Technology for Defense and Security VIII, Baltimore, Md., doi:10.1117/12.920783.

Landerer, F. W., and S. C. Swenson (2012), Accuracy of scaled GRACE terrestrial water storage estimates, *Water Resour. Res.*, *48*, W04531, doi:10.1029/2011WR011453.

Lewis, S. L., P. M. Brando, O. L. Phillips, G. M. van der Heijden, and D. Nepstad (2011), The 2010 Amazon drought, *Science*, *331*(6017), 554–554, doi:10.1126/science.1200807.

Prasad, V. K., Y. Kant, P. K. Gupta, C. Sharma, A. A. Mitra, and K. V. S. Badarinath (2001), Biomass and combustion characteristics of secondary mixed deciduous forests in Eastern Ghats of India, *Atmos. Environ.*, *35*(18), 3085–3095, doi:10.1016/S1352-2310(01)00125-X.

Randerson, J. T., G. R. Van der Werf, G. J. Collatz, L. Giglio, C. J. Still, P. Kasibhatla, J. B. Miller, J. W. C. White, R. S. DeFries, and E. S. Kasischke (2005), Fire emissions from C_3 and C_4 vegetation and their influence on interannual variability of atmospheric CO_2 and $\delta^{13}CO_2$, *Global Biogeochem. Cycles*, *19*, GB2019, doi:10.1029/2004GB002366.

Saatchi, S. S., et al. (2011), Benchmark map of forest carbon stocks in tropical regions across three continents, *Proc. Natl. Acad. Sci. U.S.A.*, *108*(24), 9899–9904, doi:10.1073/pnas.1019576108.

Soares Neto, T. G., J. A. Carvalho Jr., C. A. G. Veras, E. C. Alvarado, R. Gielow, E. N. Lincoln, T. J. Christian, R. J. Yokelson, and J. C. Santos (2009), Biomass consumption and CO_2, CO and main hydrocarbon gas emissions in an Amazonian forest clearing fire, *Atmos. Environ.*, *43*(2), 438–446, doi:10.1016/j.atmosenv.2008.07.063.

van der Werf, G. R., J. T. Randerson, L. Giglio, G. J. Collatz, M. Mu, P. S. Kasibhatla, D. C. Morton, R. S. DeFries, Y. Jin, and T. T. van Leeuwen (2010), Global fire emissions and the contribution of deforestation, savanna, forest, agricultural, and peat fires (1997–2009), *Atmos. Chem. Phys.*, *10*(23), 11,707–11,735, doi:10.5194/acp-10-11707-2010.

Ward, D. E., W. M. Hao, R. A. Susott, R. E. Babbitt, R. W. Shea, J. B. Kauffman, and C. O. Justice (1996), Effect of fuel composition on combustion efficiency and emission factors for African savanna ecosystems, *J. Geophys. Res.*, *101*(D19), 23,569–23,576, doi:10.1029/95JD02595.

Worden, H. M., M. N. Deeter, D. P. Edwards, J. C. Gille, J. R. Drummond, and P. Nédélec (2010), Observations of near-surface carbon monoxide from space using MOPITT multispectral retrievals, *J. Geophys. Res.*, *115*, D18314, doi:10.1029/2010JD014242.

Worden, J., K. Wecht, C. Frankenberg, M. Alvarado, K. Bowman, E. Kort, S. Kulawik, M. Lee, V. Payne, and H. Worden (2013a), CH_4 and CO distributions over tropical fires during October 2006 as observed by the Aura TES satellite instrument and modeled by GEOS-Chem, *Atmos. Chem. Phys.*, *13*(7), 3679–3692, doi:10.5194/acp-13-3679-2013.

Worden, J., et al. (2013b), El Niño, the 2006 Indonesian peat fires, and the distribution of atmospheric methane, *Geophys. Res. Lett.*, *40*, 4938–4943, doi:10.1002/grl.50937.

Ziehn, T., M. Scholze, and W. Knorr (2012), On the capability of Monte Carlo and adjoint inversion techniques to derive posterior parameter uncertainties in terrestrial ecosystem models, *Global Biogeochem. Cycles*, *26*, GB3025, doi:10.1029/2011GB004185.